Charge Generation and Recombination in Fullerene-Attached Poly(3-hexylthiophene)-Based Diblock Copolymer Films

ARTICLE *in* THE JOURNAL OF PHYSICAL CHEMISTRY C · MAY 2014

Impact Factor: 4.77 · DOI: 10.1021/jp4126683

8 AUTHORS, INCLUDING:

Keisuke Tajima
RIKEN
105 PUBLICATIONS **3,905** CITATIONS
SEE PROFILE

Kazuhito Hashimoto
The University of Tokyo
529 PUBLICATIONS **29,596** CITATIONS
SEE PROFILE

THE JOURNAL OF PHYSICAL CHEMISTRY C

Article

pubs.acs.org/JPCC

Charge Generation and Recombination in Fullerene-Attached Poly(3-hexylthiophene)-Based Diblock Copolymer Films

Shunsuke Yamamoto,[†,⊥] Hiroaki Yasuda,[†] Hideo Ohkita,*[,†,‡] Hiroaki Benten,[†] Shinzaburo Ito,[†] Shoji Miyanishi,[§,@] Keisuke Tajima,[‡,∥] and Kazuhito Hashimoto[§]

[†]Department of Polymer Chemistry, Graduate School of Engineering, Kyoto University, Nishikyo-ku, Kyoto, Katsura 615-8510, Japan

[‡]Japan Science and Technology Agency (JST), PRESTO, 4-1-8 Honcho Kawaguchi, Saitama 332-0012, Japan

[§]Department of Applied Chemistry, School of Engineering, The University of Tokyo, 7-3-1 Hongo, Bunkyo-ku, Tokyo 113-8656, Japan

[∥]RIKEN Center for Emergent Matter Science (CEMS), 2-1 Hirosawa, Wako, Saitama 351-0198, Japan

Supporting Information

ABSTRACT: The charge generation and recombination dynamics in fullerene-attached poly(3-hexythiophene) (P3HT)-based diblock copolymer were studied in comparison with those in blend films of P3HT and a fullerene derivative (PCBM) in order to understand the potential advantage of diblock copolymer-based polymer solar cells. Upon photoexcitation, P3HT singlet excitons are promptly converted to P3HT polarons with a time constant of ∼30 ps in both P3HT-PCBM diblock copolymer and P3HT/PCBM blend films. This similar charge generation dynamics is indicative of analogous phase-separated morphology both in these films on a scale of nanometers. After the charge generation, a part of polarons in disorder phases geminately recombine to the ground state in diblock copolymer films, while no geminate recombination is observed in blend films. This geminate recombination loss is probably due to defects of phase-separated structures in diblock copolymer films. On the other hand, charge carrier lifetime is as long as 15 μs in diblock copolymer films. Such a long carrier lifetime may result in a relatively high fill factor in P3HT-PCBM copolymer films. Finally, we discuss the overall device performance in terms of phase-separated structures.

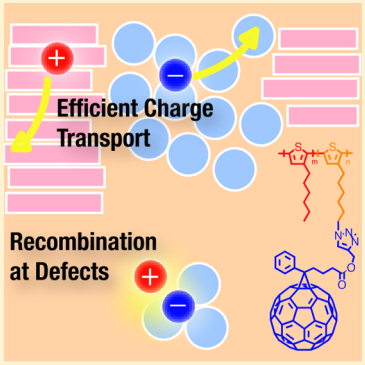

1. INTRODUCTION

Polymer/fullerene solar cells have been intensively studied and have made rapid progress in the past decade. As a result, a power conversion efficiency (PCE) of more than 10% is reported by several groups.[1,2] Bulk heterojunction blend structures are one of the keys to success in polymer/fullerene solar cells.[3] In the optimized devices, bulk heterojunction structures would provide large interface area of heterojunction to generate free charge carriers efficiently and a bicontinuous blend morphology to transport charge carriers to each electrode efficiently at the same time. In general, however, it is difficult to obtain such optimized phase-separated blend morphology spontaneously. In order to design such optimized phase-separated structures, donor−acceptor diblock copolymer-based polymer solar cells have been proposed because of its unique microphase-separated structures such as cylinder, lamella, and gyroid. For example, fullerene-attached block copolymers have been reported even in the early 2000s.[4−8] Alternatively, some block copolymers have been incorporated with a different acceptor moiety such as perylene bisimide or benzothiadiazole units instead of fullerenes.[9−12] However, most of the block copolymer-based polymer solar cells exhibit unclear microphase-separated structures and hence poor device performances, which do not exceed that of the counterpart bulk heterojunction blend solar cells. Furthermore, little is known about photophysics and charge carrier dynamics in block copolymer films. Thus, it is difficult to discuss the advantages and disadvantages of diblock copolymer structures. Very recently, it has been reported that polymer solar cells based on fullerene-attached poly(3-hexylthiophene) diblock copolymers (P3HT-PCBM) exhibit clear microphase-separated structures and efficient photovoltaic performance, which is comparable to that based on blends of poly(3-hexythiophene) (P3HT) and [6,6]-phenyl-C_{61}-butyric acid methyl ester (PCBM) (Figure 1, panels a and b).[13,14]

Herein, we study the charge generation and recombination dynamics in P3HT-PCBM copolymer films (Figure 1c) by transient absorption spectroscopy in order to understand the potential advantage of diblock copolymer-based polymer solar cells. As reported previously,[14] this P3HT-PCBM copolymer solar cell exhibits efficient device performance: J_{SC} = 8.1 mA cm^{-2}, V_{OC} = 0.48 V, FF = 0.63, and PCE = 2.5%. Of particular importance is that J_{SC} and FF are remarkably higher than those of diblock copolymer-based polymer solar cells previously reported but rather comparable to those of P3HT/PCBM blend solar cells. These device performances are indicative of

Received: December 27, 2013
Revised: May 1, 2014
Published: May 2, 2014

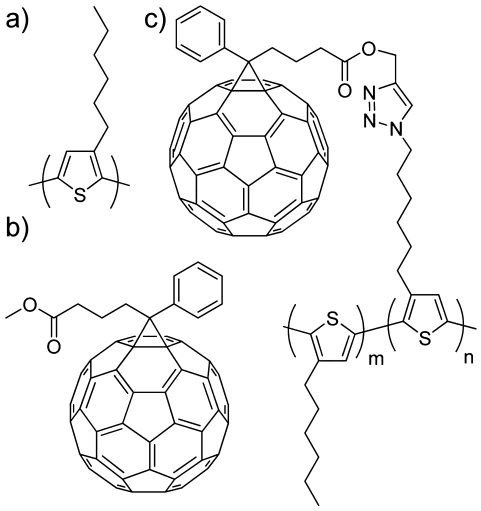

Figure 1. Chemical structures of (a) P3HT, (b) PCBM, and (c) P3HT-PCBM (m: n = 89:11) employed in this study.

efficient charge generation and transport even in P3HT-PCBM diblock copolymer films. Compared with the charge generation and recombination dynamics in P3HT/PCBM blends, we discuss the design rule for further improvement in the device performance of P3HT-PCBM diblock copolymer-based polymer solar cells.

2. EXPERIMENTAL SECTION

The P3HT-PCBM diblock copolymer was synthesized as reported previously.[13,14] Note that the device performance of this copolymer is summarized in the Supporting Information.[14] The copolymer films were fabricated by spin-coating on quartz substrates from a chlorobenzene solution of P3HT-PCBM. The quartz substrates were preliminarily treated with a UV−O_3 cleaner (Nippon Laser & Electronics, NL-UV253S) for 30 min. These fabricated films were annealed in an N_2-filled glovebox at 180 °C for 180 min. For comparison, blend films were fabricated by spin-coating on the quartz substrates from a chlorobenzene solution of P3HT (Aldrich) and PCBM (Frontier Carbon, 99.9%) with a weight ratio of 1.0:0.6, which is the same as that of P3HT-PCBM copolymer films. The blend films were annealed in an N_2-filled glovebox at 130 °C for 40 min. The film thickness was 70 nm. Absorption and fluorescence spectra of these films were measured with a UV−visible−near-IR spectrophotometer (Hitachi, U-3500) and a spectrofluorometer (Hitachi, F-4500), respectively. Transient absorption of these sample films was measured in a nitrogen atmosphere over the time range from picosecond to microsecond with two laser systems, which have been described in the Supporting Information.[15−18]

3. RESULTS AND DISCUSSION

First, we measured the absorption and fluorescence spectra of P3HT/PCBM blend and P3HT-PCBM copolymer films to discuss the blend morphology. As shown in Figure 2 (panels a and b), vibrational absorption shoulders observed at around 500−650 nm can be analyzed by a weakly interacting H-aggregate model[19] (the broken gray lines in the figure) and hence are ascribed to the $\pi-\pi$ stacking due to P3HT crystallization. The remaining absorption at around 450 nm is mainly ascribed to P3HT amorphous domains. From the absorption ratio between the crystalline and amorphous region,

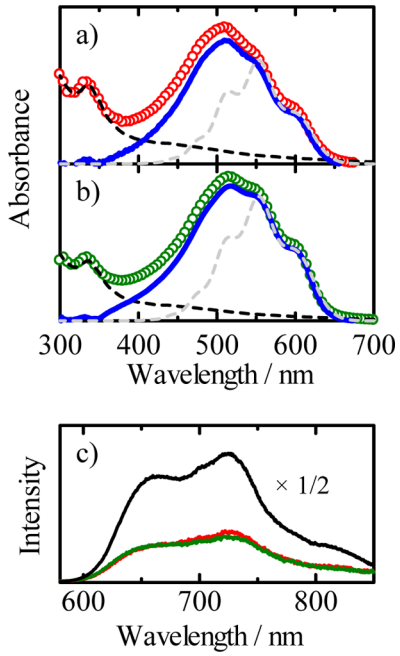

Figure 2. Absorption spectra of (a) P3HT/PCBM blend and (b) P3HT-PCBM copolymer films (○). The absorption spectra observed are resolved into the absorption of PCBM (black broken lines) and P3HT (blue solid lines). The absorption of crystalline P3HT is also estimated by the weakly interacting H-aggregate model as shown by the gray broken lines. (c) Fluorescence spectra of P3HT neat (black), P3HT/PCBM blend films (red), and P3HT-PCBM copolymer (green) excited at 400 nm.

the degree of crystallinity χ_C can be estimated by the following equation:

$$\chi_C = (\varepsilon_{460}/\varepsilon_{600})A_{600}/\{(\varepsilon_{460}/\varepsilon_{600})A_{600} + A_{460}\} \quad (1)$$

where A_{460} and A_{600} are the absorbance at 460 (amorphous) and 600 nm (crystalline) and $\varepsilon_{460}/\varepsilon_{600}$ (= 0.719) is the extinction coefficient ratio between the amorphous and crystalline P3HT.[19] As a result, the degree of P3HT crystallinity χ_C is estimated to be 36% (P3HT/PCBM blend films) and 46% (P3HT-PCBM copolymer films). On the other hand, as shown in Figure 2c, the fluorescences of these blend and copolymer films were quenched compared to that of a P3HT neat film. The quenching efficiency Φ_q was estimated to be 83% (P3HT/PCBM blend films) and 81% (P3HT-PCBM copolymer films) as summarized in Table 1, considering the excitation fraction of

Table 1. Degree of Crystallinity χ_C, Fluorescence Quenching Yield Φ_q, and Charge Carrier Lifetime τ_C of Blend and Diblock Copolymer Films

	χ_C (%)	Φ_q (%)	τ_C (μs)
blend	36	83	9
copolymer	46	81	15

P3HT in the films upon the excitation at 400 nm. These results are indicative of the similar blend morphology both in P3HT/PCBM blend and P3HT-PCBM copolymer films.

Next, we measured the transient absorption spectra of the P3HT/PCBM blend and P3HT-PCBM copolymer films to discuss the charge generation dynamics, as shown in Figure 3 (panels a and b). Here, we focus on the charge generation dynamics upon the excitation at 400 nm. Note that the charge

dx.doi.org/10.1021/jp4126683 | J. Phys. Chem. C 2014, 118, 10584−10589

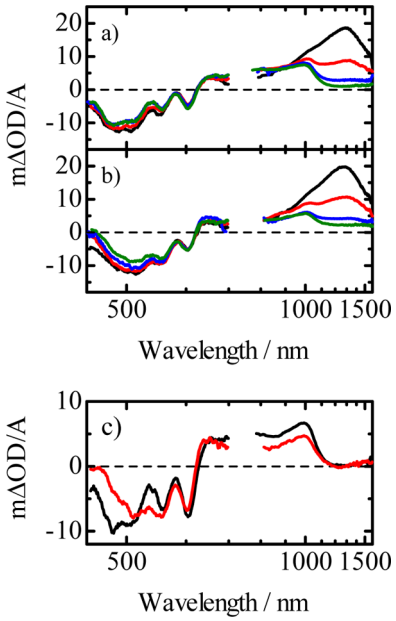

Figure 3. Transient absorption spectra of (a) P3HT/PCBM blend and (b) P3HT-PCBM copolymer films 0 ps (black), 10 ps (red), 50 ps (blue), and 100 ps (green) after the later excitation at 400 nm. The fluence was set to 5 μJ cm^{-2}. The broken lines show the baseline. (c) The transient absorption spectra of P3HT/PCBM blend (black) and P3HT-PCBM copolymer films (red) measured at 3 ns. The transient signals were corrected for variation in the absorption at the excitation wavelength.

generation dynamics upon the excitation at 500 nm cannot be discussed in detail because more than half of the excitons are deactivated to the ground state through the singlet−singlet exciton annihilation (see the Supporting Information).[15] Immediately after the laser excitation, a large absorption band was observed at around 1200 nm for both films, which is safely ascribed to the P3HT singlet exciton as reported previously.[15,16] This band disappeared in tens of picoseconds and instead broad absorption bands were observed over 650−1100 nm. These bands are ascribed to P3HT polarons as reported previously.[15,16] Note that PCBM radical anions are not observed because of its low extinction coefficient.[17] The negative signals observed over 480−610 nm are ascribed to the ground-state photobleaching, which is indicative of the generation of photoexcitations such as excitons and charge carriers to reduce the ground-state population. On the other hand, the charge generation from PCBM singlet excitons would be highly efficient, as reported previously.[20] As shown in Figure 4 (panels a and b), the decay dynamics of exciton signals is monitored at 1200 nm and the rise dynamics of polaron signals is extracted by the following relationship:

$$\Delta OD_{polaron} = \Delta OD_{1000} - \varepsilon_{1000}/\varepsilon_{1200}\Delta OD_{1200} \quad (2)$$

where $\varepsilon_{1000}/\varepsilon_{1200}$ (=0.506) is the ratio of extinction coefficients of the singlet exciton at 1000 and 1200 nm, which is estimated from the transient absorption spectra of singlet excitons in a P3HT neat film (see the Supporting Information). Note that spectral evolution of singlet excitons has negligible effect on this analysis. These transient signals are fitted by multiexponential functions as follows:

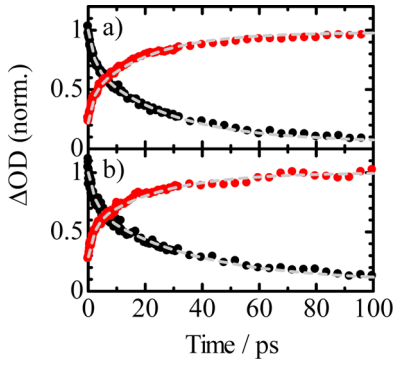

Figure 4. Time evolution of transient absorption signals of singlet excitons (black ●) and polarons (red ●) of (a) P3HT/PCBM blend and (b) P3HT-PCBM copolymer films after the laser excitation at 400 nm with a fluence of 5 μJ cm^{-2}. The gray broken lines show the fitting lines by eqs 3 and 4.

$$\Delta OD_{singlet} = A_1 \exp(-t/\tau_1) + A_2 \exp(-t/\tau_2) + A_3 \exp(-t/\tau_f) \quad (3)$$

$$\Delta OD_{polaron} = B_1\{1 - \exp(-t/\tau_3)\} + B_2\{1 - \exp(-t/\tau_4)\} + B_3 \quad (4)$$

where τ_1 to τ_4 are rise and decay time constants and τ_f is the fluorescence lifetime of P3HT (330 ps from TCSPC measurement in an N_2 atmosphere). As a result, almost the same time constants (~2 and ~30 ps) are found in the rise and decay dynamics for both films. As discussed previously, we assigned the shorter time constant and the constant fraction to the prompt charge generation at disordered domains where P3HT and PCBM are intermixed or at the interface of P3HT and PCBM domains and the longer time constant to the delayed charge generation following after the exciton diffusion into the interface. These similar charge generation dynamics are again indicative of analogous blend morphology both in the P3HT/PCBM blend and the P3HT-PCBM copolymer films on a scale of nanometers. This is fully consistent with the similar absorption and fluorescence quenching mentioned above. On a timescale of nanoseconds, singlet excitons completely disappeared and, instead, only P3HT polarons were observed. Thus, the polaron band at 3 ns is a good measure of the generation yield of free charge carriers escaping from geminate recombination. As shown in Figure 3c, the charge generation yield is smaller by 35% in P3HT-PCBM copolymer films than in the P3HT/PCBM blend upon the excitation of P3HT amorphous domains (at 400 nm). On the other hand, such charge generation loss is negligible upon the excitation of P3HT crystalline domains (at 500 nm) (see the Supporting Information). Therefore, we conclude that the overall generation loss is 20% at most, considering the crystallinity of the films (~40%). This is consistent with the device performance previously reported: the EQE and absorption spectra suggest that the charge generation efficiency in P3HT-PCBM copolymer films is almost the same at around 500−650 nm but slightly lower at around <450 nm compared to that in P3HT/PCBM blend films.[14]

In order to address the origin of the charge generation loss, we focus on the dynamics of the photobleaching signals. At 100 ps after the laser excitation, as shown in Figure 3, the P3HT singlet exciton band completely disappears and, instead, only

dx.doi.org/10.1021/jp4126683 | J. Phys. Chem. C 2014, 118, 10584−10589

P3HT polaron bands are observed. Therefore, the photobleaching signals at this time stage are safely ascribed to P3HT polarons alone, and hence, as mentioned above, the photobleaching signal at 480 nm is ascribed to polarons in disordered amorphous domains and that at 610 nm is ascribed to polarons in ordered crystalline domains. As shown in the figure, the photobleaching signal at 480 nm recovered while that at 610 nm was rather enhanced with time, suggesting that polaron dynamics is dependent on the blend morphology. Figure 5

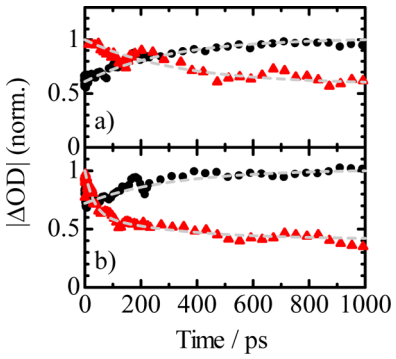

Figure 5. Transient absorption decay in the (a) P3HT/PCBM blend and (b) P3HT-PCBM copolymer films probed at 480 (red ▲) and 610 nm (black ●) after the laser excitation at 400 nm with a fluence of 5 μJ cm^{-2}. The gray broken lines show the fitting lines by exponential functions.

(panels a and b) show the time evolution of the polaron dynamics observed at 480 (amorphous phase) and 610 (crystalline phase) nm. The time evolution is fitted by multiexponential functions

$$\Delta OD_{600} = C_1[1 - \exp(-t/\tau_{cry})] + C_2 \quad (5)$$

$$\Delta OD_{480} = D_1 \exp(-t/\tau_{a1}) + D_2 \exp(-t/\tau_{a2}) + D_3 \quad (6)$$

with parameters summarized in the Supporting Information. For P3HT/PCBM blend film, the polaron dynamics at 480 nm is fitted by the sum of an exponential decay function with a time constant of τ = 300 ps (41%) and a constant fraction (59%). The polaron dynamics at 610 nm is also fitted by the sum of an exponential rise function with the same parameters: a time constant of τ = 300 ps (40%) and a constant fraction (60%). We therefore conclude that this spectral shift is attributed to the hole transfer from amorphous to crystalline P3HT domains with a time constant of τ = 300 ps. This is consistent with our previous report,[16] in which a similar hole transport is observed for P3HT/PCBM blends. For P3HT-PCBM copolymer films, on the other hand, the polaron dynamics at 480 nm is fitted by the sum of two exponential decay functions with time constants of τ = 300 ps (22%) and τ = 31 ps (36%) and a constant fraction (42%). The polaron dynamics at 610 nm is fitted by the sum of an exponential rise function with a time constant of τ = 300 ps (29%) and a constant fraction (71%). We therefore ascribe the common time constant τ = 300 ps to the hole transfer from amorphous to crystalline P3HT domains as is the case with P3HT/PCBM blend films. On the other hand, the decay constant of τ = 31 ps suggests that there is another decay pathway to the ground state because no corresponding rise fraction is found in the polaron band at 610 nm. This decay cannot be ascribed to decay of P3HT singlet excitons because no corresponding decay fraction is found in the singlet exciton band of P3HT neat films. Rather, this decay fraction (36%) is in good agreement with the reduction in the charge carrier yield compared to that of the blend film (35%), as mentioned above. We therefore conclude that this additional decay is ascribed to the geminate recombination of P3HT polarons and PCBM radical anions in amorphous domains. Note that this rapid geminate recombination (~30 ps) is much faster than that observed for the interfacial CT state isolated in RRa-P3HT/PCBM blends reported previously (~0.8 ns).[16] Rather, a similar geminate recombination with a time constant of 30 ps has been reported for micelle structures in films of P3HT terminated at one end by a fullerene.[21] Thus, we speculate that this rapid geminate recombination also results from such micellelike structures formed as defects of microphase-separated structures in P3HT-PCBM copolymer films. Furthermore, this rapid decay fraction is in good agreement with the reduction in the polaron generation at 3 ns. We therefore conclude that the rapid recombination results in the reduced polaron yield. In contrast, no geminate recombination was observed for P3HT/PCBM blend films. This is consistent with our previous report.[16]

We now move onto the charge carrier dynamics on a timescale of microseconds under a continuous white light bias of 100 mW cm^{-2}. Here we roughly estimate the charge carrier lifetime τ_C from the pseudo-first order recombination of laser-induced charge carriers, as reported previously.[18,22,23] Figure 6

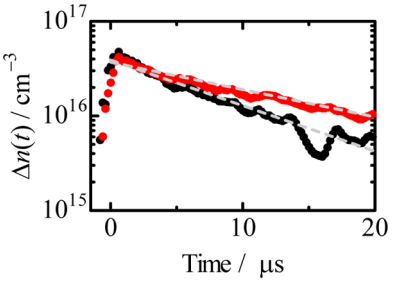

Figure 6. Microsecond transient absorption decay in P3HT/PCBM blend (black) and P3HT-PCBM copolymer films (red) probed at 1000 nm after the laser excitation at 500 nm with a fluence of 0.3 μJ cm^{-2} under continuous white light bias with 100 mW cm^{-2}. The gray broken lines show the fitting lines by the pseudo-first-order kinetics $\Delta n(t) = n_0 \exp(-t/\tau_C)$ with a time constant τ_C of 9 (P3HT/PCBM blend films) and 15 (P3HT-PCBM copolymer films) μs, respectively.

shows the microsecond transient absorption decay with continuous white light bias. The charge carrier lifetime τ_C can be roughly estimated from the pseudo-first order recombination dynamics of laser-induced charge carriers as reported previously.[18] As a result, τ_C is estimated to be 9 μs (P3HT/PCBM blend films) and 15 μs (P3HT-PCBM copolymer films). Note that the charge carrier lifetime is longer in the copolymer film than in the blend film, even without the white light bias (see the Supporting Information).[24,25] Such longer carrier lifetime suggests that P3HT domains are well-segregated from PCBM domains because of microphase-separated structures in the copolymer film. Indeed, lamellarlike phase-separated domains with a periodic structure of ~10 nm have been reported for the P3HT-PCBM copolymer films previously.[13] Furthermore, the longer lifetime indicates that the micellelike defects as mentioned above do not serve as bimolecular recombination centers, though they serve as

dx.doi.org/10.1021/jp4126683 | J. Phys. Chem. C 2014, 118, 10584−10589

geminate recombination centers. This is probably because electron of PCBM radical anions cannot transfer to isolated PCBM domains in the micelle structure because of the surrounding P3HT chains. In other words, the bimolecular recombination is effectively suppressed by microphase-separated structures but independent of the micellelike defects in P3HT-PCBM copolymer films.

Finally, we summarize the relevance of the charge generation and recombination dynamics studied here to the overall device performance. In the charge generation, 35% of P3HT polarons in disordered domains geminately recombine to the ground state with a time constant of 31 ps in P3HT-PCBM copolymer films while no geminate recombination is observed in the P3HT/PCBM blend films. This geminate recombination loss is probably due to micellelike defects in microphase-separated structures. On the other hand, the charge carrier lifetime on a timescale of microseconds is longer in P3HT-PCBM copolymer films than in P3HT/PCBM blend films. This is probably because clear phase-separated morphology in diblock copolymer films would reduce bimolecular recombination. The longer carrier lifetime is desirable for the efficient charge collection in the device because the charge mobility is likely to be similar or higher in P3HT-PCBM than in P3HT/PCBM, considering the higher crystallinity of P3HT-PCBM copolymer films. Such longer charge carrier lifetime and high mobility may be the origin of the high fill factor, even in diblock copolymer-based solar cells. Therefore, the key to success for diblock copolymer-based solar cells is to suppress micellelike defects that would cause geminate recombination loss.

4. CONCLUSION

We studied the charge generation and recombination dynamics in P3HT-PCBM copolymer films by transient absorption spectroscopy in order to understand the potential advantage of diblock copolymer-based polymer solar cells. In the charge generation, 35% of P3HT polarons in disordered domains geminately recombine to the ground state in P3HT-PCBM copolymer films, while no geminate recombination is observed in P3HT/PCBM blend films. This geminate recombination loss is probably due to micellelike defects in microphase-separated structures. In contrast, such charge generation loss is negligible upon the excitation of P3HT crystalline domains (at 500 nm). We therefore conclude that the overall generation loss is 20% at most, considering the crystallinity of the films (~40%). On the other hand, the charge carrier lifetime is longer in P3HT-PCBM copolymer films than in P3HT/PCBM blend films. Such a longer carrier lifetime is desirable for the efficient charge collection in the device. As a result, the overall device performance would be comparable between the two polymer solar cells. We therefore conclude that diblock copolymer-based solar cells have potential advantage to exceed bulk heterojunction blend solar cells. The key to success for diblock copolymer-based solar cells is to suppress micellelike defects that would cause geminate recombination loss.

■ ASSOCIATED CONTENT

Supporting Information

Complete author list for refs 2 and 12, detailed setup for transient absorption measurements, device parameters, transient absorption spectrum of singlet excitons in P3HT, detailed kinetic parameters for transient decay analyses, transient absorption spectra upon excitation at 500 nm, and bimolecular recombination dynamics. This material is available free of charge via the Internet at http://pubs.acs.org.

■ AUTHOR INFORMATION

Corresponding Author

*E-mail: ohkita@photo.polym.kyoto-u.ac.jp. Tel: +81 75 383 2613. Fax: +81 75 383 2617.

Present Addresses

[⊥]S.Y.: Institute of Multidisciplinary Research for Advanced Materials (IMRAM), Tohoku University, 2-1-1 Katahira, Aoba-ku, Sendai 980-8577, Japan.

[@]S.M.: Chemical Resources Laboratory, Tokyo Institute of Technology, R1-17, 4259 Nagatsuta, Midori-ku, Yokohama 226-8503, Japan.

Notes

The authors declare no competing financial interest.

■ ACKNOWLEDGMENTS

This work was partly supported by the JST PRESTO program (Photoenergy Conversion Systems and Materials for the Next Generation Solar Cells) and the New Energy and Industrial Technology Development Organization (NEDO), Japan.

■ REFERENCES

(1) Green, M. A.; Emery, K.; Hishikawa, Y.; Warta, W.; Dunlop, E. D. Solar Cell Efficiency Tables (version 42). *Progress in Photovoltaics: Research and Applications* **2013**, *21*, 827−837.

(2) You, J.; Dou, L.; Yoshimura, K.; Kato, T.; Ohya, K.; Moriarty, T.; Emery, K.; Chen, C.-C.; Gao, J.; Li, G.; et al. A Polymer Tandem Solar Cell with 10.6% Power Conversion Efficiency. *Nat. Commun.* **2013**, *4*, 1446.

(3) Yu, G.; Gao, J.; Hummelen, J. C.; Wudl, F.; Heeger, A. J. Polymer Photovoltaic Cells: Enhanced Efficiencies via a Network of Internal Donor-Acceptor Heterojunctions. *Science* **1995**, *270*, 1789−1791.

(4) Venkataraman, D.; Yurt, S.; Venkatraman, B. H.; Gavvalapalli, N. Role of Molecular Architecture in Organic Photovoltaic Cells. *J. Phys. Chem. Lett.* **2010**, *1*, 947−958.

(5) Roncali, J. Single Material Solar Cells: the Next Frontier for Organic Photovoltaics? *Adv. Energy Mater.* **2011**, *1*, 147−160.

(6) Ramos, A.; Rispens, M.; van Duren, J.; Hummelen, J. C.; Janssen, R. A. J. Photoinduced Electron Transfer and Photovoltaic Devices of a Conjugated Polymer with Pendant Fullerenes. *J. Am. Chem. Soc.* **2001**, *123*, 6714−6715.

(7) Tan, Z.; Hou, J.; He, Y.; Zhou, E.; Yang, C.; Li, Y. Synthesis and Photovoltaic Properties of a Donor-Acceptor Double-Cable Polythiophene with High Content of C_{60} Pendant. *Macromolecules* **2007**, *40*, 1868−1873.

(8) Yang, C.; Lee, J. K.; Heeger, A. J.; Wudl, F. Well-Defined Donor−Acceptor Rod−Coil Diblock Copolymers Based on P3HT Containing C_{60}: The Morphology and Role as a Surfactant in Bulk-Heterojunction Solar Cells. *J. Mater. Chem.* **2009**, *19*, 5416−5423.

(9) Lindner, S. M.; Hüttner, S.; Chiche, A.; Thelakkat, M.; Krausch, G. Charge Separation at Self-Assembled Nanostructured Bulk Interface in Block Copolymers. *Angew. Chem., Int. Ed.* **2006**, *45*, 3364−3368.

(10) Rajaram, S.; Armstrong, P.; Kim, B. J.; Fréchet, J. M. J. Effect of Addition of a Diblock Copolymer on Blend Morphology and Performance of Poly(3-hexylthiophene): Perylene Diimide Solar Cells. *Chem. Mater.* **2009**, *21*, 1775−1777.

(11) Sommer, M.; Komber, H.; Huettner, S.; Mulherin, R.; Kohn, P.; Greenham, N. C.; Huck, W. T. S. Synthesis, Purification, and Characterization of Well-Defined All-Conjugated Diblock Copolymers PF8TBT-*b*-P3HT. *Macromolecules* **2012**, *45*, 4142−4151.

(12) Johnson, K.; Huang, Y.-S.; Huettner, S.; Sommer, M.; Brinkmann, M.; Mulherin, R.; Niedzialek, D.; Beljonne, D.; Clark, J.; Huck, W. T. S.; et al. Control of Intrachain Charge Transfer in Model

Systems for Block Copolymer Photovoltaic Materials. *J. Am. Chem. Soc.* **2013**, *135*, 5074−5083.
(13) Miyanishi, S.; Zhang, Y.; Tajima, K.; Hashimoto, K. Fullerene Attached All-Semiconducting Diblock Copolymers for Stable Single-Component Polymer Solar Cells. *Chem. Commun.* **2010**, *46*, 6723−6725.
(14) Miyanishi, S.; Zhang, Y.; Hashimoto, K.; Tajima, K. Controlled Synthesis of Fullerene-Attached Poly(3-alkylthiophene)-Based Copolymers for Rational Morphological Design in Polymer Photovoltaic Devices. *Macromolecules* **2012**, *45*, 6424−6437.
(15) Guo, J.; Ohkita, H.; Benten, H.; Ito, S. Near-IR Femtosecond Transient Absorption Spectroscopy of Ultrafast Polaron and Triplet Exciton Formation in Polythiophene Films with Different Regioregularities. *J. Am. Chem. Soc.* **2009**, *131*, 16869−16880.
(16) Guo, J.; Ohkita, H.; Benten, H.; Ito, S. Charge Generation and Recombination Dynamics in Poly(3-hexylthiophene)/Fullerene Blend Films with Different Regioregularities and Morphologies. *J. Am. Chem. Soc.* **2010**, *132*, 6154−6164.
(17) Yamamoto, S.; Guo, J.; Ohkita, H.; Ito, S. Formation of Methanofullerene Cation in Bulk Heterojunction Polymer Solar Cells Studied by Transient Absorption Spectroscopy. *Adv. Funct. Mater.* **2008**, *18*, 2555−2562.
(18) Yamamoto, S.; Ohkita, H.; Benten, H.; Ito, S.; Yamamoto, S.; Kitazawa, D.; Tsukamoto, J. Efficient Charge Generation and Collection in Amorphous Polymer-Based Solar Cells. *J. Phys. Chem. C* **2013**, *117*, 11514−11521.
(19) Clark, J.; Chang, J.-F.; Spano, F. C.; Friend, R. H.; Silva, C. Determining Exciton Bandwidth and Film Microstructure in Polythiophene Films Using Linear Absorption Spectroscopy. *Appl. Phys. Lett.* **2009**, *94*, 163306.
(20) Cook, S.; Katoh, R.; Furube, A. *J. Phys. Chem. C* **2009**, *113*, 2547−2552.
(21) Banerji, N.; Seifter, J.; Wang, M.; Vauthey, E.; Wudl, F.; Heeger, A. J. Ultrafast Spectroscopic Investigation of a Fullerene Poly(3-hexylthiophene) Dyad. *Phys. Rev. B* **2011**, *84*, 075206.
(22) Maurano, A.; Shuttle, C. G.; Hamilton, R.; Ballantyne, A. M.; Nelson, J.; Zhang, W.; Heeney, M.; Durrant, J. R. Transient Optoelectronic Analysis of Charge Carrier Losses in a Selenophene/Fullerene Blend Solar Cell. *J. Phys. Chem. C* **2011**, *115*, 5947−5957.
(23) Credgington, D.; Durrant, J. R. Insights from Transient Optoelectronic Analyses on the Open-Circuit Voltage of Organic Solar Cells. *J. Phys. Chem. Lett.* **2012**, *3*, 1465−1478.
(24) More correctly, the charge carrier lifetime τ_n is given by $\tau_n = (1 + \lambda)\tau_C$, where λ can be evaluated from the exponent in the power-law decay of charge carriers as reported in ref 25. Details are described in the Supporting Information.
(25) Shuttle, C.; Ballantyne, A.; Nelson, J.; Bradley, D.; Durrant, J. Bimolecular Recombination Losses in Polythiophene: Fullerene Solar Cells. *Phys. Rev. B* **2008**, *78*, 113201.